



NRC Publications Archive Archives des publications du CNRC

Formation and properties of C-S-H -PEG nano-structures

Beaudoin, J. J.; Dramé, H.; Raki, L.; Alizadeh, R.

This publication could be one of several versions: author's original, accepted manuscript or the publisher's version. / La version de cette publication peut être l'une des suivantes : la version prépublication de l'auteur, la version acceptée du manuscrit ou la version de l'éditeur.

For the publisher's version, please access the DOI link below. / Pour consulter la version de l'éditeur, utilisez le lien DOI ci-dessous.

Publisher's version / Version de l'éditeur:

<https://doi.org/10.1617/s11527-008-9439-x>

Materials and Structures, 42, 7, pp. 1003-1014, 2009-07-01

NRC Publications Record / Notice d'Archives des publications de CNRC:

<https://nrc-publications.canada.ca/eng/view/object/?id=5993b0cd-ec25-4f65-9871-7442d4f96cfd>

<https://publications-cnrc.canada.ca/fra/voir/objet/?id=5993b0cd-ec25-4f65-9871-7442d4f96cfd>

Access and use of this website and the material on it are subject to the Terms and Conditions set forth at

<https://nrc-publications.canada.ca/eng/copyright>

READ THESE TERMS AND CONDITIONS CAREFULLY BEFORE USING THIS WEBSITE.

L'accès à ce site Web et l'utilisation de son contenu sont assujettis aux conditions présentées dans le site

<https://publications-cnrc.canada.ca/fra/droits>

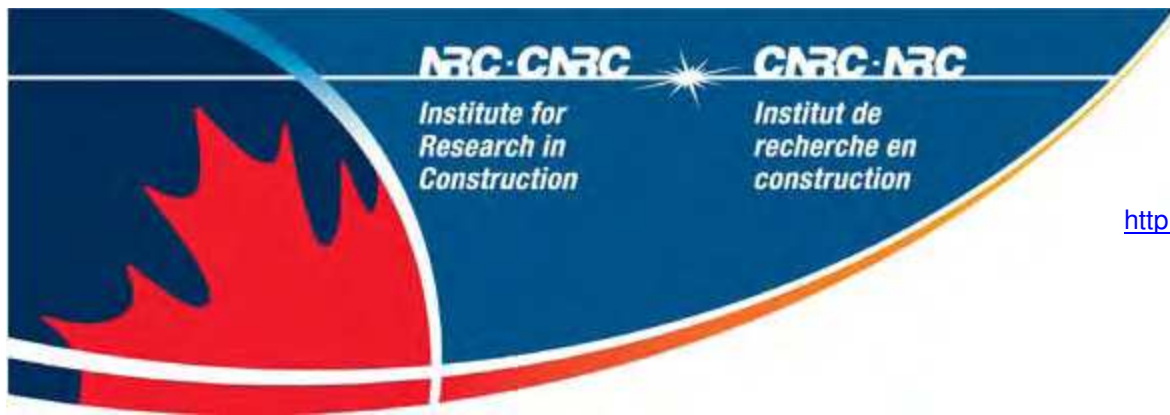
LISEZ CES CONDITIONS ATTENTIVEMENT AVANT D'UTILISER CE SITE WEB.

Questions? Contact the NRC Publications Archive team at

PublicationsArchive-ArchivesPublications@nrc-cnrc.gc.ca. If you wish to email the authors directly, please see the first page of the publication for their contact information.

Vous avez des questions? Nous pouvons vous aider. Pour communiquer directement avec un auteur, consultez la première page de la revue dans laquelle son article a été publié afin de trouver ses coordonnées. Si vous n'arrivez pas à les repérer, communiquez avec nous à PublicationsArchive-ArchivesPublications@nrc-cnrc.gc.ca.





Formation and properties of C-S-H -PEG nano-structures

NRCC-51315

Beaudoin, J.J.; Dramé, H.; Raki, L.; Alizadeh, R.

July 2009

A version of this document is published in / Une version de ce document se trouve dans:
Materials and Structures, 42, (7), pp. 1003-1014, DOI: [10.1617/s11527-008-9439-x](http://dx.doi.org/10.1617/s11527-008-9439-x)

The material in this document is covered by the provisions of the Copyright Act, by Canadian laws, policies, regulations and international agreements. Such provisions serve to identify the information source and, in specific instances, to prohibit reproduction of materials without written permission. For more information visit <http://laws.justice.gc.ca/en/showtdm/cs/C-42>

Les renseignements dans ce document sont protégés par la Loi sur le droit d'auteur, par les lois, les politiques et les règlements du Canada et des accords internationaux. Ces dispositions permettent d'identifier la source de l'information et, dans certains cas, d'interdire la copie de documents sans permission écrite. Pour obtenir de plus amples renseignements : <http://lois.justice.gc.ca/fr/showtdm/cs/C-42>



National Research
Council Canada

Conseil national
de recherches Canada

Canada 

FORMATION AND PROPERTIES OF C-S-H -PEG NANO-STRUCTURES

James J. Beaudoin*, Harouna Dramé, Laila Raki and Rouhollah Alizadeh

Institute for Research in Construction, National Research Council of Canada

M-20, 1200 Montreal Road, Ottawa, Ontario K1A 0R6, Canada

** E-mail: jim.beaudoin@nrc-cnrc.gc.ca, Tel: 613-993-6749; Fax: 613-954-5984*

Abstract

Results of an investigation of the intercalation potential of polyethylene glycol (PEG) with synthetic and pre-treated C-S-H are reported. The partial intercalation of PEG molecules in the interlayer of C-S-H is discussed. The effective and strong interaction of PEG molecules with the C-S-H surface was shown using XRD, ^{13}C CP and ^{29}Si MAS NMR, and DTGA. The position and character of the 002 low angle XRD peak of C-S-H are affected by drying procedures and concomitant chemical treatment preceding intercalation and the reaction temperature. Recovery of the initial 002 position after severe drying and intercalation with distilled water or PEG is incomplete but is accompanied by an increase in intensity. It is inferred that the stability of C-S-H binders in concrete can be impacted by a variation in nanostructure dependent on curing temperature and use of chemical admixtures.

Keywords: Calcium Silicate Hydrate (C-S-H), intercalation, organic solvents, PEG, nanostructure

INTRODUCTION

The volume stability of hydrated Portland cement and concrete is central to durability issues concerning exposure to aggressive media [1]. Disruptive expansions often occur in concert with deleterious reactions between hydrated cement phases (or cement minerals themselves) and ions in the pore solution present as a result of various transport processes [2-4].

Recently clay scientists have had considerable interest in the volume stability and formation of organomineral derivatives because they combine the structural, physical and chemical properties of both the inorganic host material and the organic guest species at a nanometer scale [5-10]. Methods based on the modification of pre-existing inorganic structures offer considerable potential for the design of new hybrid nanocomposites of interest to the construction and building material industries. The intercalation of organic molecules is well established in clay mineralogy and related layered structures [11-16].

The development of new cement-based materials and the determination of their suitability for practical application is a multistep process. The investigation of organic/inorganic cement composites as potential candidates for innovative applications in construction is in its infancy. The first step in the process is to identify suitable candidate polymers and study their interactions with basic binding materials such as C-S-H. Subsequent steps would include physico-chemical and physico-mechanical measurements to assess engineering behavior. Durability assessment would follow. The use of helium gas as a nanostructural probe is an example of how the 'tightness' of the composite system might be assessed. The specific objective of this work is related to the first step and is to assess the merits and

nature of the C-S-H-PEG interaction. This polymer was chosen following an analysis of the clay science literature.

The ultimate research question is essentially, “Are materials based on the C-S-H-PEG interactions viable candidates for use in the construction industry?” The short term goal is to take the first step in the process described above. The initial approach is to synthesize and characterize the C-S-H-PEG composites. This would be followed by engineering measurements (e.g. elastic modulus, strength, dynamic response). The potential resistance of these systems to the transport of aggressive ions would then be determined. A helium diffusion technique, referred to above, would be employed. It would be expected that the polymer would inhibit the flow of helium gas under pressure into the nanostructure of the C-S-H.

There is a paucity of durability related information available on the understanding of synthetic calcium silicate hydrate (C-S-H) modified with surfactants and polymers. Significant variation in its composition, nanostructure, and morphology can occur [17]. Results of a systematic study of the modification of C-S-H structure by intercalation of polyethylene glycol (PEG) with and without pretreatment with dimethyl sulfoxide (DMSO) and sodium chloride solutions are reported.

Calcium Silicate Hydrates

(C-S-H) phases are the major reaction products (50-70% by mass) and primary binding phases in hydrated Portland cement. Recent models of the nanostructure of hydrated

Portland cement describe the layered nature of the silicate phases [17-21]. Calcium silicate hydrate structure is often referred to that of tobermorite [17, 22, 23]. It has similarities to the clay minerals in crystal structure assembly [5, 22]. The composite 2:1 sheets are made up of a distorted calcium hydroxide sheet flanked on both sides by parallel rows of wollastonite-type chains having composition $\text{Ca}_4\text{Si}_6\text{O}_{18}$ [23]. The remaining or interlayer calcium atoms and water molecules reside between them. Generally, two types of calcium are considered: “nonlabile” Ca linked to silica chains and “labile” Ca linked to Si-OH (silanol) groups. C-S-H has a surface pH dependent charge due to the existence of silanol sites carried by bridging silica tetrahedra or by the end chain tetrahedra [17, 18, 22, 24].

Clay-based Structural Analogues

Clay particles are formed from aluminosilicates arranged as parallel octahedral and tetrahedral layers. These layers carry a negative surface charge density, which arises from isomorphic substitutions in the tetrahedral or in the octahedral layers. Smectite clays such as montmorillonite are expandable clays, in the sense that they have exchangeable cations (Ca^{2+} , Na^+ , K^+ , Mg^{2+}) and water molecules situated in between the layers. These ions neutralize the surface charge density on the wall and make the solid electrically neutral [25-27]. If the interlayer cations are monovalent and strongly hydrated (i.e. Na^+ , Li^+), the interplatelet repulsion is stronger and the degree of platelet separation is larger [27-29]. The extent of interlayer swelling depends on the nature of the swelling agent, the exchange cation, the charge density and the location of the layer charge. The interlayer

cations could be exchanged by many types of organic intercalates ranging from alkyl-ammonium salts to varieties of polymer having different chain length, size and geometry [6]. It is also possible to functionalize their interlamellar hydroxyl groups of clays by covalent grafting of an appropriate metal chelating ligand [30-32] as reported for the minerals kaolinite and magadiite [12, 13, 33].

Intercalation of Polymers into Layered Silicates

Polymers, in general, can be intercalated into an inorganic lamellar material by three different approaches: incorporation of a monomer followed by “*in situ*” polymerization; direct insertion of the polymer from solution or from a melt; insertion in a pre-formed substrate matrix. It has been shown that polymer melt intercalation is the most promising approach to fabricate polymer-based nanocomposites [34,35]. One of the difficulties of direct polymer intercalation is the surface compatibility between the inorganic host and the polymer. Layered aluminosilicates are organophobic. It is therefore essential to first modify the silicate to facilitate the transport of the polymer chains into their interlamellar spaces. Therefore, in most of the reported inclusion of polymers into aluminosilicate compounds, the interlamellar cations were exchanged with long-chain alkylammonium ions prior to polymer insertion [36-42]. Alkylammonium cations in the organosilicates lower the surface energy of the inorganic host and improve the wetting characteristics of the polymer matrix, and result in a larger interlayer spacing. Additionally, the alkylammonium cations can provide functional groups that can react with the polymer matrix, or in some cases initiate the polymerization of monomers to improve the strength of the interface between the inorganic host and the polymer matrix [43,44]. Depending on

the strength of interfacial interactions between the polymer and layered silicate (modified or not), three different types of polymer/layered silicate (PLS) nanocomposites are thermodynamically achievable [45]:

1. Intercalated nanocomposites: the insertion of a polymer into the layered silicate structure occurs in a crystallographically regular fashion, regardless of the inorganic host to polymer ratio. Intercalated nanocomposites normally contain a few molecular layers of polymer. Properties of the composites typically resemble those of ceramic materials.
2. Flocculated nanocomposites: conceptually these are similar to intercalated nanocomposites. However, silicate layers are sometimes flocculated due to hydroxylated “edge-edge” interaction of the silicate layers.
3. Exfoliated nanocomposites: the individual inorganic host layers are separated in a continuous polymer matrix by an average distance that depends on inorganic mineral loading. Usually, the inorganic host content of an exfoliated nanocomposite is much lower than that of an intercalated nanocomposite.

The objective of the present study is to determine to what extent the intercalation process described above is feasible or applicable to C-S-H with specific reference to PEG and DMSO molecules. The results of a study to assess the relationship between the behavior of hydrated calcium silicate and clay, upon modification with polyethylene glycol (PEG) polymers of different molecular weight, are reported. The method of C-S-H synthesis, effect of Na⁺ exchange and surfactant on intercalation, nature of organic guest intercalates, as well as the mechanism of ion interaction and specific adsorption at

surfaces will be discussed. The X-ray diffraction (XRD), ^{13}C CP MAS and ^{29}Si MAS solid state nuclear magnetic resonance (NMR) spectroscopy, and differential thermal gravimetric analysis (DTGA), were used to characterize and follow changes and behavior of the C-S-H modifications.

EXPERIMENTAL

Materials

All chemicals used were of reagent-grade quality and were not further purified unless otherwise specified.

C-S-H Synthesis

C-S-H was synthesized by mixing of CaO and reactive SiO₂ in stoichiometric proportions in distilled water (preferably decarbonated) under N₂ to avoid exposure to the atmospheric CO₂. The preparation of CaO consisted of heating pure CaCO₃ at 900°C for at least 3 hours and cooling in a N₂ atmosphere. Amorphous silica (Cabosil) was heated at 110°C for 3 hours and mixed intimately with the CaO (in 500 mL high density polypropylene bottles) to obtain a C/S molar ratio of 1.6. The required amount of demineralized decarbonated water (water/solid = 10) was added and the system was flushed with N₂ before sealing. The reaction was conducted at room temperature with the bottles rotated at the speed of 16 rpm for up to 14 days. Longer hydration periods were not studied in this investigation. The above synthesis procedure involved subjecting the slurry mixture to high speed shearing for 5 min. before placing the bottles on rotating rollers. The high speed shearing was at 6100 rpm/min. using a Silverson Laboratory

Mixer. The C-S-H was filtered under N₂ and dried under vacuum for 12 hours at various temperatures. The samples were labeled C-S-H01, C-S-H02, C-S-H03 (A and B) and C-S-H04. C-S-H01 was vacuum dried at 65°C, C-S-H02 at 70-75°C, C-S-H03A at 47-50°C, C-S-H03B at 50-60°C and C-S-H04 at 25°C. Extreme care was taken during the drying procedure to ensure the reproducibility of the results and stability of the material.

Drying of the C-S-H in this work was conducted in a temperature controlled vacuum cell using a mechanical vacuum pump (pressure= 1.33×10^{-2} Pa). The significance of drying in the context of this work relates to the relative ease with which the polymer can intercalate into the host material. Drying above 50°C (hard drying) makes this more difficult. Previous work by the authors on volume stability of C-S-H clearly shows this as expansion on wetting in distilled water is significantly reduced at drying temperatures above 50°C [46]. The PEG melt requires heating above 50°C and adds to the complexity of the process.

C-S-H Characterization

Powder x-ray diffraction (XRD):

XRD measurements were performed with a Philips PW3710 diffractometer using CuK α radiation. The powder patterns were recorded at 45kV and 40mA, using step scanning with a step size of 0.02° 2 θ at a scan rate of 0.5 ° 2 θ /min in the intervals 1.41° < 2 θ < 35°, 1.41° < 2 θ < 15° or 1.41° < 2 θ < 4° when a more detailed pattern was needed. A background subtraction correction was performed on all XRD patterns. The XRD pattern indicated the presence of the primary peaks previously reported for C-S-H (I), [47]. These were (in

order of intensity) at 'd ' values of 1.25, 0.304, 0.280 nm. A low angle peak at $d=1.82$ nm was also observed. A small residual amount of calcium hydroxide was detected.

Thermogravimetric Analysis (TGA):

A Polymer Labs STA 1500H instrument (TGA/DTA) with a nitrogen flow rate of 25 cc/min and a heating rate of 20°C/min (30-1000°C) was used. The thermogravimetric curve (mass loss versus temperature) was qualitatively and quantitatively similar to that reported by Taylor for C-S-H gel [47]. The mass loss in the region, 400-600°C, was very small for Taylor's specimen. An even smaller loss was observed for the C-S-H used in this study suggesting that the residual amount of Ca(OH)_2 is small or negligible. Constitutional water likely contributes to the small mass loss in this region.

Nuclear Magnetic Resonance

^{29}Si MAS NMR spectra were recorded at 39.7MHz on a TecMag Apollo spectrometer using a 7mm Doty probe. Chemical shifts are reported relative to an external tetramethylsilane reference sample ($\delta = 0.0$ ppm). Samples were spun in 7mm zirconia rotors at 4 kHz, and a 7 μs 90° pulse was used. The final spectra took up to 48h to obtain.

^{13}C CP MAS NMR (50.33 MHz) spectra were obtained using a Bruker ASX-200 instrument. ^{13}C CP MAS NMR spectra were referenced to the aliphatic carbons of hexamethylbenzene at $\delta = 17.2$ ppm. Samples were spun in 7mm zirconia rotors at 4 kHz, and a 7 μs 90° pulse was used. Commercial MAS probes provided by Bruker and Chemmagnetics were used.

Pre-treatment of Pre-formed C-S-H

Selected C-S-H preparations were chemically pretreated to assess their potential to accommodate organic intercalates. The treatment involved the following cation exchange and intercalation procedures:

DMSO – C-S-H

Preparation of dimethyl sulfoxide (DMSO) treated C-S-H designated DMSO – C-S-H was carried out by reacting C-S-H04 with DMSO at 25°C for 24h followed by filtration and washing with 1, 2 dioxane to remove the excess DMSO. The material was then vacuum dried at 25°C for 12h.

Na – C-S-H

Preparation of Na – C-S-H from the originally prepared C-S-H material was carried out by reacting the C-S-H04 with NaCl solutions (20 g/L and saturated) for 24 h followed by filtration and washing with distilled water until the halide (Cl) was not detected with AgNO₃. The materials were dried under vacuum at 50-60°C and labeled Na- C-S-H03B1 and Na – C-S-H03B2. In an alternate experiment an aqueous solution of NaCl (20 g/L) was used directly during C-S-H synthesis. The mixture was submitted to high-speed shear at 6100 rpm for 5 min and reacted for 6 days. The sample obtained was labeled Na – C-S-H hs6d.

C-S-H-Organic Nanocomposite Preparation

Polyethylene glycol samples of MW 300 (PEG300) and MW 1000 (PEG1000) obtained from Aldrich Chemicals was heated between 65-70°C. C-S-H03B, DMSO-C-S-H and Na-C-S-H were dispersed in the polymer melt under N₂ with vigorous magnetic stirring for 24h. At the end of the reaction run, the product was filtered and washed with methanol to remove the excess polymer. The filtered product was labeled C-S-H – PEG(300,1000), DMSO – C-S-H – PEG(300,1000), Na – C-S-H – PEG(300,1000), . The numbers in parentheses indicate the MW i.e.PEG300 or PEG1000.

Summary – Specimen Designations

A summary of the specimen designations is provided in Table 1 for easy reference.

Table 1 – Designations for C-S-H Preparation

Designation	Description
C-S-H01	Vacuum dried at 65-70°C for 12h
C-S-H02	Vacuum dried at 70-75°C for 12h
C-S-H03A	Vacuum dried at 47-50°C for 12h
C-S-H03B	Vacuum dried at 50-60°C for 12 h
C-S-H04	Vacuum dried at 25°C for 12h
Na-C-S-HO3B1	C-S-H immersed in NaCl solution (20 g/L) for 24 h and vacuum dried for 12h at 50-60°C
Na-C-S-HO3B2	C-S-H immersed in NaCl solution (saturated) for 24h and vacuum dried at 50-60°C for 12h
Na-C-S-H hs6d	NaCl solution (20 g/L) used during synthesis of of C-S-H. High speed shearing (hs) for 5 min. was used (see text) with a 6 day reaction time
DMSO-C-S-H	C-S-H 04 immersed in DMSO solution at 25°C for 24h followed by vacuum drying at 25°C for 12h
C-S-H-PEG(300,1000)	C-S-H 03B dispersed in PEG melt at 65-70°C with vigorous stirring for 24h
DMSO-C-S-H-PEG(300,1000)	DMSO-C-S-H dispersed in PEG melt at 65-70°C with vigorous stirring for 24h
Na-C-S-H- PEG(300,1000)	Na-C-S-H dispersed in PEG melt at 65-70°C with vigorous stirring

RESULTS AND DISCUSSION

The results of the various characterization techniques (XRD, ^{13}C CP MAS NMR, ^{29}Si MAS NMR, and TGA) applied to the various C-S-H preparations and test regimes are presented in the following sections.

1) XRD

1-a Effect of Drying Condition on Distilled Water Treatment of C-S-H(I).

The compositions of the C-S-H and C-S-H-based complexes were investigated using X-ray diffraction analysis. The X-ray pattern of the quasicrystalline C-S-H ($C/S = 1.6$) is characterized by well-defined peaks at approximately 0.306, 0.280 and 0.182 nm [47]. In the absence of guest molecules a (002) basal reflection at 1.25 nm is clearly detected. The pattern obtained is similar to that reported in the literature for C-S-H [47]. The 002 peak position will be used as a reference peak for the modified samples. The shape and position of the (002) peak is very sensitive to the drying conditions and methods of chemical modification. The effect of drying conditions on the (002) peak and its recovery after being in contact with distilled water (DW) for 19 days is shown in Figure 1. Curve (a) is representative of C-S-H that has been dried at temperatures below 50°C . It is considered as the reference sample. It has been shown in previous work that the volume stability of C-S-H immersed in distilled water is similar if drying temperatures do not exceed 50°C [47]. At more elevated temperatures the volume change is significantly reduced. Drying above 50°C induces significant collapse of interlayer space. This collapse of structure is evident in curves (b) and (c) as there is a shift in the (002)

reflection to $d=1.05$ nm and an effective reduction in peak intensity with increase in drying temperature. Treatment with distilled water (curve d) does not result in a recovery of the initial basal spacing (following the partial collapse at 70°C) but an increase in intensity is evident. The relevance of drying at 70°C lies in the requirement for a temperature range of $65\text{-}70^{\circ}\text{C}$ for the PEG melts.

1-b C-S-H-PEG Interaction-Pre-treatment with DMSO and NaCl Solutions

In a series of subsequent experiments the C-S-H was subjected to chemical treatment with DMSO before reaction with various polymers. The effect of DMSO treatment is shown in Figure 2. The reference in this case (curve a) is represented by C-S-H vacuum dried at $65\text{-}70^{\circ}\text{C}$. This drying temperature was chosen as the interaction of C-S-H with PEG300 and PEG1000 melts occurs at $65\text{-}70^{\circ}\text{C}$. DMSO treatment is also carried out under reflux at $50\text{-}60^{\circ}\text{C}$. The reference curve for this C-S-H preparation (DMSO-C-S-H) has a (002) reflection at $d \cong 0.98\text{nm}$ indicative of thermal treatments above 50°C .

DMSO was used to explore the capability of these small organic polar molecules to break the hydrogen bonds, if any, with the interlayer silanol groups in order to enhance the potential intercalation of the polymers e.g. PEG300 and PEG1000.

The reference C-S-H treated with PEG1000 (curve b) indicates a slight shift in the basal spacing to a higher value at $d=1.03$ nm. The DMSO treatment itself has little effect on the position of the basal spacing (curve c). The interaction of PEG300 with DMSO-C-S-H is shown in curve d. The (002) reflection is less intense than that for PEG1000 (curve e) but

the low angle peak ($d = 4.53$ nm) is significantly more intense possibly due to the presence of two phases. The curve (e), for polymer treatment of DMSO-C-S-H indicates that PEG1000 has an effect on the treated C-S-H host. The (002) peak is more intense and shifts to a higher basal spacing. There is also an indication of another low angle peak at $d = 4.33$ nm. It is inferred that DMSO treatment favors slightly the interaction of the polymer with the C-S-H.

The X-ray spectrum for Na-C-S-H 03B (not shown) has a more intense and broader peak for the basal spacing at $d=1.02$ nm compared to C-S-H(I) dried at 60°C . Pretreatment of C-S-H with both sodium chloride and DMSO solutions has potential.

1-c Low angle XRD Basal Spacings: C-S-H

A feature of all the previous XRD patterns is the presence of an additional peak at the lower angle between 1.41° and $4^{\circ} 2\theta$ ($d \cong 4.50$ nm). Analysis (after the background subtraction, curve a) of the evolution of the low angle peak after PEG treatments (Figure 3) indicates similarities (in the increase in intensity, broadening and shifting) as observed previously with the (002) peak. The increase in intensity (at $d \cong 4.50$ nm) compared to the reference C-S-H (curve b) resulting from PEG polymer interaction is evident (curves c and d). It is apparent that PEG treatment may result in a structural rearrangement resulting from partial intercalation or expansion and the development of this lower peak.

Summary

The XRD study has shown how the pretreatment with DMSO and NaCl solution, temperature and drying conditions can affect the structure of C-S-H, and the extent of

intercalation of guest molecules between the layers. This result is in agreement with the study of Cong et al. [48], that shows the inappropriateness of oven drying C-S-H at 110°C because at this temperature not only does the layered structure collapse, but the polymerization of silicate chains is also changed. In this study it has been shown that vacuum drying over 50°C and even prolonged vacuum drying at ambient temperatures have a similar effect on the C-S-H structure. It is suggested that if possible mild vacuum drying without any source of heat should be used (depending on the amount of wet sample being treated) in order to preserve the structure of the hydrate.

¹³C CP MAS NMR and ²⁹Si MAS NMR

¹³C CP MAS NMR spectra of DMSO-C-S-H (Figure 4) preparations were obtained in order to investigate structural properties of the organic component in this organo-calcium silicate hydrate. Figure 4 provides evidence of the effective presence of DMSO guest molecules in the treated C-S-H matrix. A significant ¹³C resonance signal of DMSO appears at 40.30 ppm corresponding to one of the two methyl groups. Another signal appears at 168.55 ppm. It may be due to the presence of slight carbonation during the reaction or to the formation of another carbonyl compound. It is noteworthy that when DMSO is intercalated into kaolinite, for example, two ¹³C methyl resonance signals are observed. In the present case with C-S-H, we have observed only one ¹³C methyl signal. In clay systems, it is reported that one ¹³C methyl signal is observed only when DMSO is co-intercalated into kaolinite with oxyethylene species [49,50].

The dipolar dephasing technique was applied. The ratio of I_{DD}/I_0 , where I_{DD} and I_0 are the peak intensities of the ¹³C resonance obtained respectively with and without dipolar

dephasing conditions, is a semi quantitative measure of the dynamic state of the molecular group [51-53]. If a molecular group is rigidly bound, the ratio I_{DD}/I_0 will be decreased. The overall signal decay for carbons strongly coupled to protons, such as methylene carbons has been shown to be best described by the following equation [52]:

$$I_{DD} = I_0 e^{-\tau^2 / (2T_2^3)}$$

where τ is the dipolar dephasing delay time and T_2 is the transverse relaxation time constant.

^{13}C CP MAS and DD CP MAS (dipolar dephasing) experiments were performed on DMSO-C-S-H-PEG300 (Figure 5a, b) in order to obtain information regarding the interlayer structure and dynamics of the intercalated DMSO-C-S-H host.

The PEG polymer was found to be relatively mobile since after 40 μs of dipolar dephasing a significant signal could still be detected. The sharp and intense signal at 168 ppm is likely due to carbonation occurring during the preparation or to the formation of some carbonyl compound.

^{29}Si MAS NMR

^{29}Si MAS NMR was used to assess the effect of sodium and DMSO pretreatment on the nanostructure of C-S-H. The spectra of C-S-H, Na-C-S-H, and Na-C-S-H-DMSO are presented in Figure 6. In all cases, the spectra are dominated by a doublet (Q^1 , Q^2) located respectively at (-79.3, -85.2 ppm), (-79.7, -85.9 ppm) and (-79.3, -84.8 ppm) in Figure 6-a, 6-b and 6-c, respectively. These two resonances are characteristic of silicate

dreierketten feature of the C-S-H structure. The Q^2/Q^1 ratio, used to determine the mean chain length for the silicate entities present in the structure, increases significantly with sodium pretreatment but reverts back to the reference value when sodium and DMSO treatment are combined. This observation implies that the polymerization state of silicates is affected by the sodium pretreatment but not by the combination of sodium and DMSO. The spectra for C-S-H-PEG300, C-S-H-PEG450 and C-S-H-PEG1000 (numbers refer to PEG molecular weight) are presented in Figure 7. The Q^2/Q^1 ratio increases significantly for the C-S-H-PEG nanohybrids relative to the control C-S-H indicating that PEG treatment results in much larger silicate chains.

Grafting at sites of missing tetrahedra has been reported for silylated polymers [54]. It is known that electrons of the atoms in the vicinity of existing $-O-Si-O$ bonds can shield the silicon nuclei resulting in a detectable chemical shift. These shifts depend on the extent and strength of shielding. A chemical shift for the silicon atom will occur in the following cases: $-O-Si-O-H$; $-O-Si-O-Na$; $-O-Si-O-Si-$; $-O-Si-O-[Polymer]$. The chemical shift is different most of the time but it is theoretically possible to have two different attachments that result in a similar chemical shift. In other words the chemical shift of Si in the vicinity of the polymer can be similar to that obtained with a Si-O-Si bond and mimic the latter which is called Q^2 . This would explain the increase in the Q^2/Q^1 ratio observed for C-S-H-PVA by Matsuyama and Young [55]. A schematic of the C-S-H structure showing possible sites for polymer grafts is provided in Figure 8.

DTGA

The DTGA curves for PEG and DMSO modified C-S-H are shown in Figure 9. All the samples have a low temperature peak corresponding to the weight loss at about 138°C and two peaks at 353°C and 410°C corresponding respectively to the surface adsorbed DMSO and PEG, and the dehydroxylation of C-S-H. The total weight loss in this region is 3.8% for DMSO – C-S-H, 7.12% DMSO – C-S-H – PEG300 and 8.6% DMSO – C-S-H – PEG1000. This result indicates the simultaneous presence of DMSO and PEG. The peak corresponding to a small third weight loss appears in polymer modified samples DMSO – C-S-H – PEG300 and DMSO – C-S-H – PEG1000 and is located at 558°C. Corresponding weight losses are 3.4 and 3.8% respectively for DMSO – C-S-H – PEG300 and DMSO – C-S-H – PEG1000. Peaks representing two other weight losses are located at about 679°C for all samples and about 800°C for PEG modified samples. It is important to mention that in the case of C-S-H modified by DMSO, the first weight loss due to the removal of physisorbed water occurs at a lower temperature compared to that in the reference C-S-H.

These weight loss results show that all the modified C-S-H samples contain organic guest molecules. The presence of weight losses at elevated temperatures of 667°C, 773°C and 905°C suggests that part of polymer is intercalated in the interlayer space of C-S-H.

It is evident that the intercalation of DMSO and PEG into the interlamellar space of C-S-H has dramatically altered the decomposition sequence of C-S-H. This is seen in the reduced temperatures of C-S-H dehydroxylation as well as the appearances of additional weight losses at 383, 555, 800 and 904°C. Structural reorganization occurs above 830°C

and up to 914°C for the analyzed samples. The structural collapse followed by the complete dehydroxylation of the C-S-H itself appears to cause the residual interlayer carbonaceous material to be trapped within a meta – C-S-H like matrix, forming a carbon-calcium silicate nanocomposite material. Some of this carbonaceous material may be released once the material undergoes this structural reorganization between 800-1000°C. Combustion in air occurs relatively fast and a weight loss not normally associated with a structural reorganization is observed [12].

CONCLUSIONS

The present study has shown how the temperature and drying conditions affect the structure and ability of C-S-H to accommodate (partially) DMSO and PEG intercalates between the layers. The results show that vacuum drying over 50°C and even prolonged vacuum drying at 25°C lead to a collapse of the interlayer space of the C-S-H structure. The effect of the reaction temperature during the intercalation of high molecular weight polymer is also significant. It is suggested that mild vacuum drying without any source of heat be used in order to preserve the structure of the hydrate. The study has shown that depending on the drying conditions and the pretreatment with DMSO and NaCl solution, intercalation of PEG into the interlayer space of pre-formed C-S-H is possible. The importance of defining a (002) peak reference position (XRD) before making any assessment of possible intercalation is recommended in order to take into account the effect of the intercalation temperature and drying condition on the host structure relative to the available interlayer gallery height. For each drying condition, a shift in the (002)

peak position occurs. Relative intercalation from a predetermined starting position can be observed.

The present study has provided evidence (based on DTGA) that the adsorption and intercalation of DMSO and PEG polymers on the surface and into the interlamellar spaces of C-S-H can dramatically alter the thermal decomposition behavior of C-S-H. This was reflected in the reduced temperatures of C-S-H dehydroxylation as well as the appearances of additional weight losses at 383, 555, 800 and 904°C. Structural reorganization occurs above 830°C and up to 914°C for analyzed samples with weight loss thought to be the result of the release of carbonaceous materials trapped within a meta-C-S-H-like matrix. The modified thermal behavior of the C-S-H in presence of PEG provides evidence (supplementing that obtained by other techniques) that the polymer is associated with a true nanocomposite. All data are consistent with the structural integrity of C-S-H being maintained after organic modification. It can be inferred from this study that the curing temperature, the degree of hydration, and the presence of chemical and mineral admixtures in Portland cement-based materials can significantly influence the nature of the C-S-H composition, nanostructure, and morphology. An understanding of these processes could have meaningful impact on the long-term durability of concrete structures. Further, it is suggested that tailoring the nanostructure of C-S-H-based materials offers a potential route for the realization of durability strategies.

REFERENCES

1. P. W. BROWN, H. F. W. TAYLOR, in “Materials Science of Concrete: Special Volume on Sulfate Attack Mechanisms”, edited by J. Marchand and J.P. Skalny (American Ceramic Society, 2000) p. 73.
2. J. MARCHAND, “Modeling the behavior of unsaturated cement systems exposed to aggressive chemical environments” *Mater. Struct.* 34 (2001) 195-200.
3. H. F. W. TAYLOR, C. FAMY and K. SCRIVENER, “Delayed ettringite formation” *Cem .Concr.Res.* 31 (2001) 683-693.
4. G. G. LITVAN, “Volume stability of porous solids. Part I.” in Proceedings of the 7th International Congress on Chemistry of Cement, Paris, France, 1980, Vol. 3, p. VII-46-VII-46-VII-50.
5. J. A. RAUSSELL-COLOM, and M. J. SERRAIOUSA, in “Chemistry of Clays and Clay Minerals”, Edited by A.C.D. Newman. (Mineralogical Society, London, 1987) p. 371.
6. T. J. PINNAVAIA, “Intercalated clay catalysts” *Science.* 220,4595, (1983) 365-371.
7. A. OKADA, M. KAWASUMI, A. USUKI, A., Y. KOJIMA, T. KURAUCHI and O. KAMIGAITO, “ Synthesis and properties of nylon-6/clay hybrids” in

- Proceedings MRS Symposium on Polymer-based Molecular Composites,
Edited by D. W. Schaefer and J. E. Mark, Vol. 171 (1990) p. 45-50.
8. R. A. VAIA, G. PRICE, P. N. RUTH, H. T. NGUYEN AND J. LICHTENHAN, "Polymer/layered silicate nanocomposites as high performance ablative materials" *Appl. Clay Sci.* 15 (1999) 67-92.
 9. M. BISWAS and R. S. SINHA, "Recent progress in synthesis and evaluation of polymer-montmorillonite nanocomposites" *Adv. Polym. Sci.*, 155 (2001) 167-221.
 10. SINHA, R.S., YAMADA, K., OKAMOTO, M., UEDA, K., "New polylactide/ layered silicate nanocomposite: a novel biodegradable material", *Nano Lett.* 2,1093-1096, (2002).
 11. H. VAN OLPHEN, in "An introduction to Clay and Colloid Chemistry" (John Wiley & Sons, New York 1977) p 318.
 12. J. J. TUNNEY and C. DETELLIER, "Interlammellar covalent grafting of organic units on kaolinite" *Chem. Mater.* 5 (1993) 747-748.
 13. J. J. TUNNEY and C. DETELLIER, "Preparation and characterization of an 8.4 Å hydrate kaolinite" *Clays and Clay Miner.* 42 (1994) 552-560.
 14. B. VELDE, in "Introduction to Clay Minerals" (Chapman and Hall, Ed., London, 1992) p 195.

15. W. DOSCH, “Interlamellar reaction of tetracalcium aluminate hydrates with water and organic compounds” in Proceedings of the 15th National Conference on Clay and Clay Minerals, Pittsburgh, PA, (1966) p 273-292.
16. V. H. TERISSE, A. NONAT and C. J. PETIT, “Zeta potential study of calcium silicate hydrates interacting with alkaline cations” *J. Coll. Int. Sc.* 244 (2001) 58-65.
17. G. I. RICHARDSON, “ Tobermorite/jennite and tobermorite/calcium hydroxide-based models for the structure of C-S-H: applicability to hardened pastes of tricalcium silicate, β - dicalcium silicate, Portland cement and blends of Portland cement with blast furnace slag, metakaolin or silica fume” *Cem. Concr. Res.* 34, (2004) 1733-1777.
18. ALIZADEH R., BEAUDOIN, J.J., RAKI L. “C-S-H (I) - A Nanostructural model for the removal of water from hydrated cement paste,” *Journal of the American Ceramic Society*, 90 (2007) 670–672.
19. A. J. ALLEN, J.J. THOMAS and H. JENNINGS, “ Composition and density of nanoscale calcium- silicate- hydrate in cement” *Nature Materials* 6 (2007) 311-316.
20. R. F. FELDMAN and P. J. SEREDA, “The new model for hydrated Portland cement and its practical implications” *Eng. J.* 53 (1970) 53-57.
21. H. F. W. TAYLOR, in “Cement Chemistry”(Academic Press, London , 1990) p 475.

22. S. A. HAMID, "The crystal structure of the 11 Å tobermorite $\text{Ca}_{2.25}[\text{Si}_3\text{O}_{7.5}(\text{OH})_{1.5}] \cdot \text{H}_2\text{O}$ " *Z. Kristallogr.* 154 (1981) 189-198.
23. R. F. FELDMAN and P. J. SEREDA, "A model for hydrated Portland cement paste as deduced from sorption-length change and mechanical properties" *Matériaux et Construction.* 1 (1968) 509-520.
24. J. J. BEAUDOIN, "Why engineers need materials science" *Concrete Int.* 21 (1999) 86-89.
25. H. VAN OLPHEN, in "An Introduction to Clay Colloid Chemistry" (Wiley, 2nd Edition, 1997) p 318.
26. M. B. MCBRIDE, in "Environmental Chemistry of Soils" (Oxford University Press, 1994) p 416.
27. B. VELDE, in "Introduction to clay minerals: chemistry, origins, uses and environmental significances" (Chapman and Hall, 1st Edition, 1992) p 195.
28. A.C.D. NEWMAN, in "Chemistry of clays and clay minerals" (Monograph No. 6, Mineralogical Society, 1987) p 480.
29. P. F. LUCKHAM and S. ROSSI, "The colloidal and rheological properties of bentonite suspensions" *Adv. Coll. Interf. Sc.* 82 (1999) 43-92.
30. H. DEUEL, "Organic derivatives of clay minerals" *Clay Miner. Bull.* 1 (1952) 205-214.

31. H. DEUEL, “ Reaktionen von silikaten mit organischen verbindungen”
Macromol. Chem. 34 (1959) 206-215.
32. B. EVANS and T. E. WHITE, “ Adsorption and reaction of
methylchlorosilane at an ‘Aerosil’ surface” J. Catal. 11 (1968) 336-341.
33. T. YANAGISAWA, K. KURODA and C.KATO, “ Organic derivatives of
layered polysilicates I. Trimethylsilylation of magadite and kenyaite” React.
Solids, 5, 167-175, (1988).
34. R. A. VAIA, H. ISHII and E. P. GIANNELIS, “ Synthesis and properties of
two dimensional nanostructures by direct intercalation of polymer melts in
layered silicates” Chem. Mat. 5 (1993) 1694-1696.
35. P. ARNANDA and E. RUITZ-HITZKY, “ Poly(ethyleneoxide)-silicate
intercalation materials” Chem. Mat. 4 (1992) 1395-1413.
36. G. LAGALY, M. FERNADEZ and A. WEISS, “ Problems in layers-charge
determination of montmorillonite” Clays and Clay Minerals 50 (1976) 435-
445.
37. W. F. JAYNES and S. A. BOYD, “Clay minerals type and organic compound
sorption by hexadecyletrymethyl- ammonium exchanged clays” Soil Sci. Soc.
Amer. J. 55 (1991) 43-48.

38. D.M.C., MACEWEN, “ Complexes of clays with organic compounds: 1. Complex formation between montmorillonite and halloysite and certain organic liquids” *Trans. Fara. Soc.* 44 (1984) 349-367.
39. A. WEISS, “ Organic derivatives of mica-type layer silicates” *Ange. Chem. Inter.* 2 (1963) 134-144.
40. Z. WANG, T. LAN . and J. PINNAVAIA, “ Hybrid organic-inorganic nanocomposites formed from an epoxy polymer and a layered silicic acid (magadrite)” *Chem. Mater.* 8 (1996) 2200-2204.
41. Y. SUGAHARA, M. SUGIMOTO, T. YANAGISAWA, Y. NOMIZU, K. KURODA and C. J. KATO, “The preparation of magadite-polyacrylonitrile intercalation compound and its conversion to silicon carbide” *Ceram. Soc. Jpn. Int. Ed.* 95 (1987) 109-114.
42. Z. WANG, T. LAN and T. J. PINNAVAIA, “ Hybrid organic-inorganic nanocomposites: exfoliation of magadite nanolayers in an elastomeric epoxy polymer” *Chem. Mater.* 10 (1998) 1820-1826.
43. A. BLUMSTEIN, “ Polymerization of adsorbed monolayers: II Thermal degradation of the inserted polymers” *J. Polym. Sci, A.* 3 (1965) 2665-2673.
44. R. KRISHNAMOORTI, VAIA RA and E. P. GIANNELIS, “ Structure and dynamics of polymer-layered silicate nanocomposites” *Chem Mater.* 8 (1996) 1728-1734.

45. R. S. SINHA, K. OKAMOTO and M. OKAMOTO, “ Structure property relationship in biodegradable poly (butylene succinate)/ layered silicate nanocomposites” *Macromolecules*. 36 (2003) 2355-2367.
46. H. DRAMÉ, J. J. BEAUDOIN and L. RAKI, “ Structure property relationship in biodegradable poly (butylene succinate)/layered silicate nanocomposites” *J. Mater. Sc.* 42 (2007) 6846-6848.
47. H.F.W. Taylor, “Proposed structure of calcium silicate gel”, *J. Amer. Ceram. Soc.* 69(6) (1986) 464-467.
48. X. CONG and R. J. KIRKPATRICK, “ Effects of the temperature and relative humidity on the structure of C-S-H gel” *Cem. Concr. Res.* 25 (1995) 1237-1245.
49. M. RAUPACH, P. F. BARRON and J. G. THOMPSON, . “ Nuclear Magnetic Resonance, Infrared and X-ray powder diffraction study of dimethylsulfoxide and dimethylselenoxide intercalates with kaolinite” *Clays Clay Miner.* 35 (1987) 208-219.
50. J. G. THOMPSON and C. CUFF, “Crystal structure of kaolinite: dimethylsulfoxide intercalate” *Clays Clay Miner.* 33 (1985) 490-500.
51. L. B. ALEMANY, D. M. GRANT, T. D. ALGER and R. J. PUGMIRE, “Cross-polarization and magic angle spinning NMR spectra of model organic compounds 3. Effect of ^{13}C - ^1H dipolar interaction on cross-polarization and carbon proton dephasing” *J. Am. Chem. Soc.* 105 (1983) 6697-6704.

52. S. J. OPELLA and M. H. FREY, "Selection of protonated carbon resonances in solid state nuclear magnetic resonance" *J. Am. Chem. Soc.* 101 (1979) 5954-5956.
53. J. A. RIPMEESTER and N. E. BURLINSON, " Chiral discrimination and solid state ^{13}C NMR. Application to tri-o-thymotide clathrates" *J. Am. Chem. Soc.* 107 (1985) 3713-3714.
54. A. FRANCESCHINI, S. ABRAMSON, B. BRESSON, H. VANDAMME and N. LEQUEUX, "Cement-silylated polymers nanocomposites," *Proc. 12th Int. Cong. Chem. Cem. Theme ST5, Montreal, July 08-13, 2007.*
55. H. MATSUYAMA and J.F.Young, "Intercalation of polymers in calcium silicate hydrate: A new synthetic approach to biocomposites" *Chem. Mater.* 11, 16-19, 1999.

FIGURE CAPTIONS

- Fig. 1. The effect of C-S-H drying condition on the position of the 002 XRD peak and its recovery following immersion in distilled water (19d). Curves: (a) C-S-H03A vacuum dried 12h at 47-50°C; (b) C-S-H03B vacuum dried 12h at 60-65°C; (c) C-S-H02, vacuum dried 12h at 70°C; (d) C-S-H02-DW immersed in DW 19d and vacuum dried 12h at 25°C; C-S-H designations are described in detail in Table 1.
- Fig. 2. The effect of DMSO treatment on the interaction of C-S-H with PEG polymers. XRD curves: (a) C-S-H01; (b) C-S-H-PEG1000, (c) DMSO-C-S-H; (d) DMSO-C-S-H-PEG300, (e) DMSO-C-S-H-PEG1000; C-S-H designations are described in detail in Table 1.
- Fig. 3 Evolution of low angle XRD peak (about $2.15^{\circ}2\theta$) for PEG polymer treated C-S-H. XRD curves: (a) background; (b) C-S-H03B (vacuum dried at 60-65°C for 12h); (c) C-S-H03B-PEG1000 (vacuum dried at 25°C for 12h); (d) C-S-H03B-PEG300 (vacuum dried at 25°C for 12h); C-S-H designations are described in detail in Table 1.
- Fig. 4 ^{13}C CP MAS NMR spectra of DMSO-C-S-H.
- Fig. 5 ^{13}C CP MAS NMR spectra of DMSO-C-S-H-PEG 300: (a) regular CP MAS spectrum; (b) dipolar dephasing spectrum.

Fig. 6 ^{29}Si MAS NMR spectra of: (a) C-S-H04; (b) Na-C-S-H04; (c) DMSO-C-S-H04; C-S-H designations are described in detail in Table 1.

Fig. 7 ^{29}Si MAS NMR spectra of: (a) C-S-H-PEG450; (b) C-S-H-PEG1000; (c) C-S-H-PEG300. Numbers refer to PEG molecular weight.

Fig. 8 A schematic of C-S-H nanostructure showing possible sites for PEG polymer grafts.

Fig. 9 DTGA curves for DMSO modified C-S-H before and after interaction with PEG polymers. C-S-H designations are described in detail in Table 1.

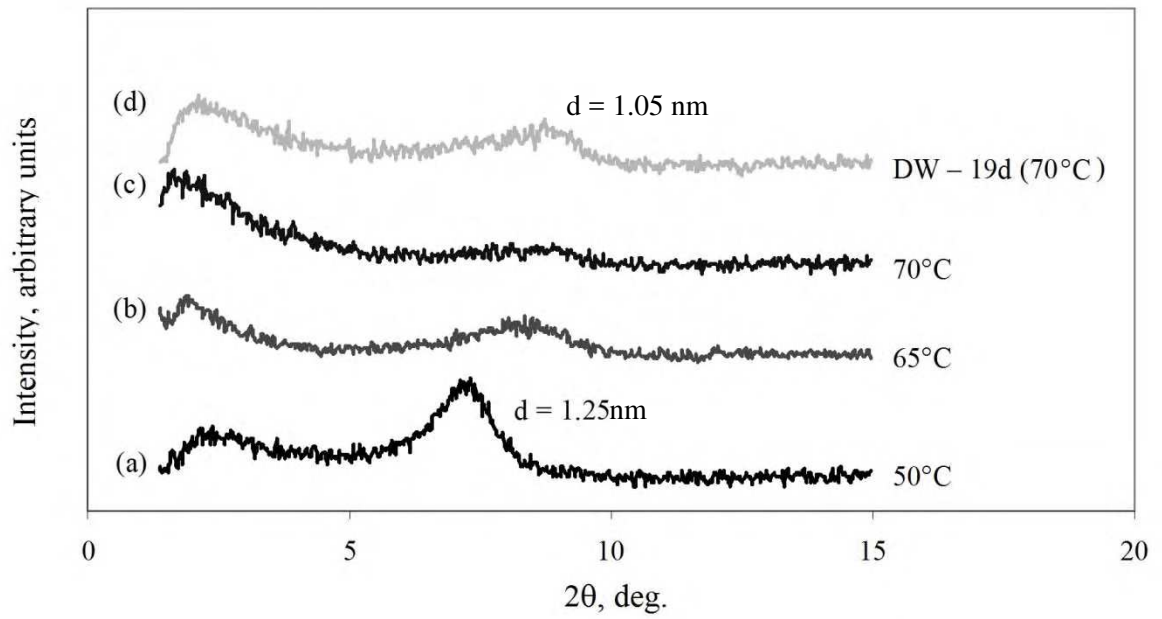


Figure 1

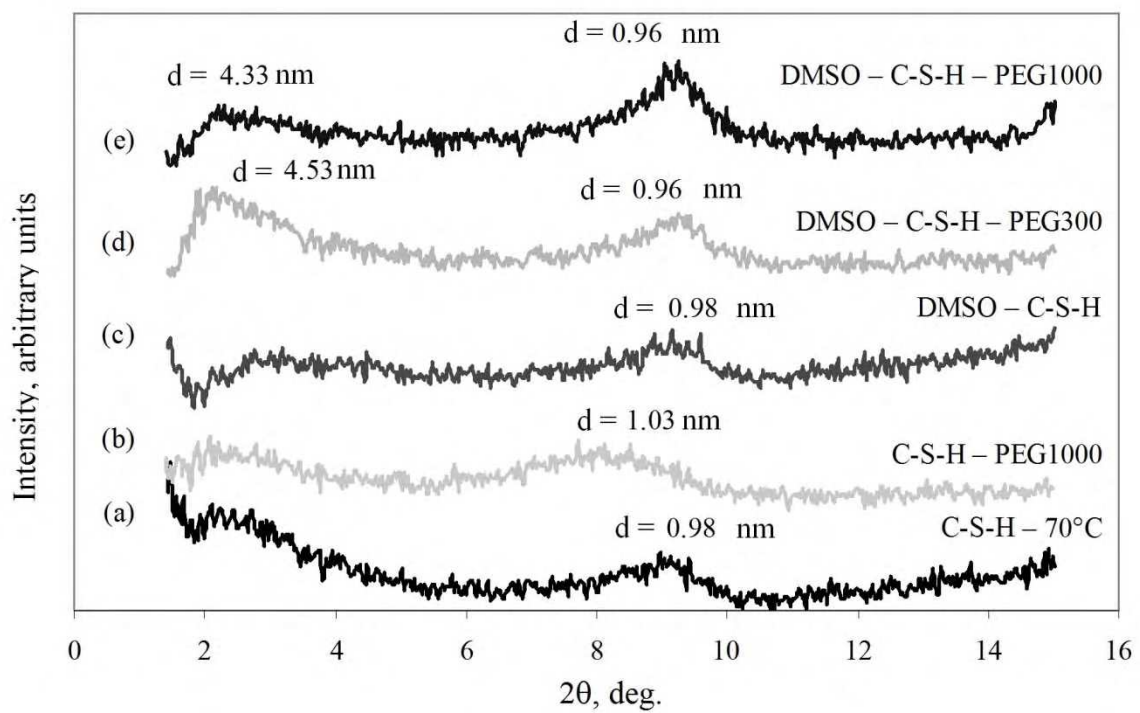


Figure 2

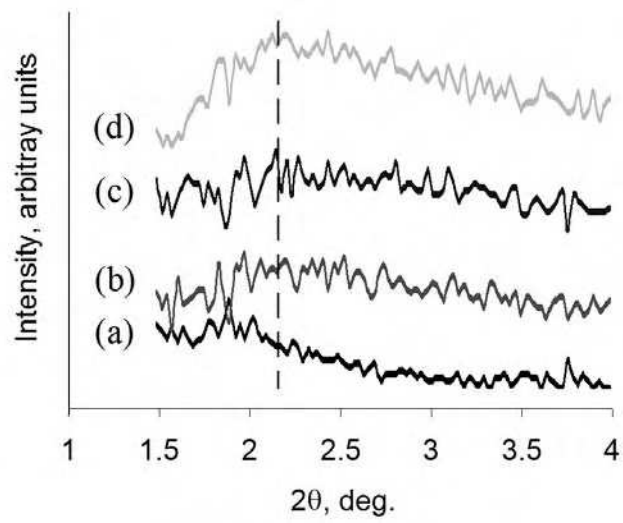


Figure 3

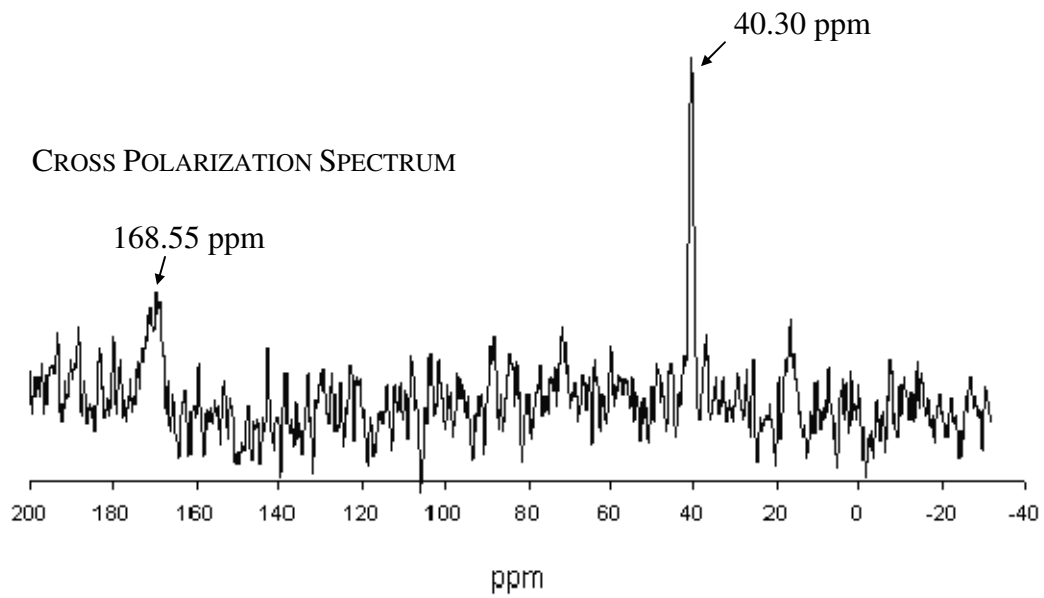


Figure 4

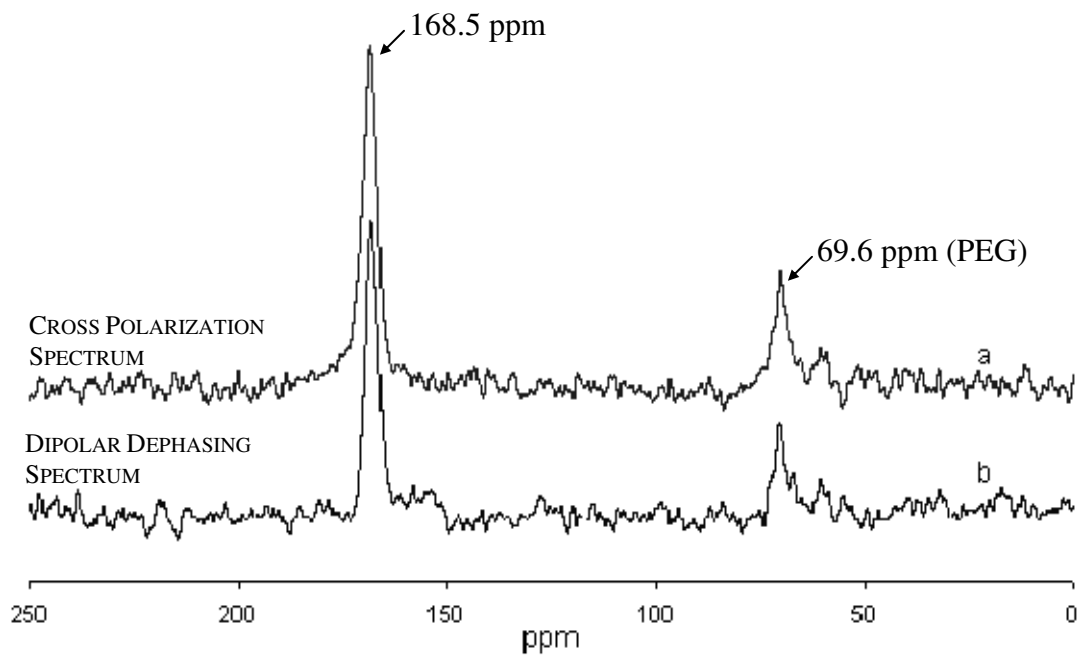


Figure 5

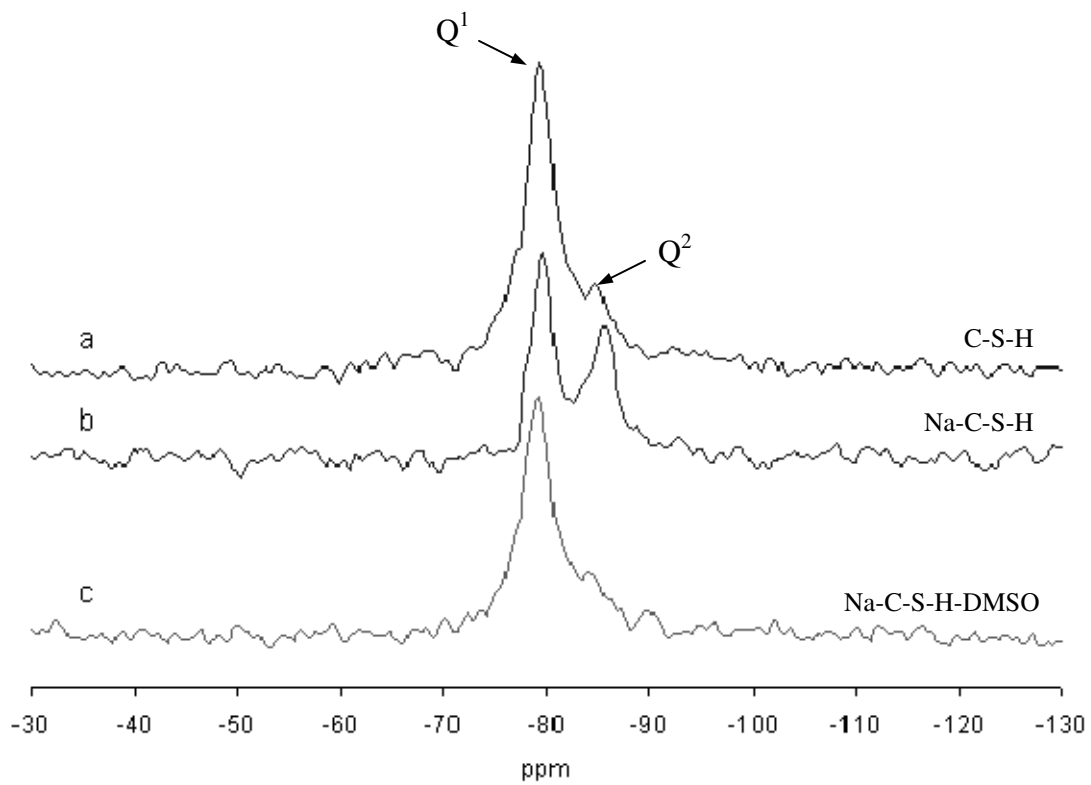


Figure 6

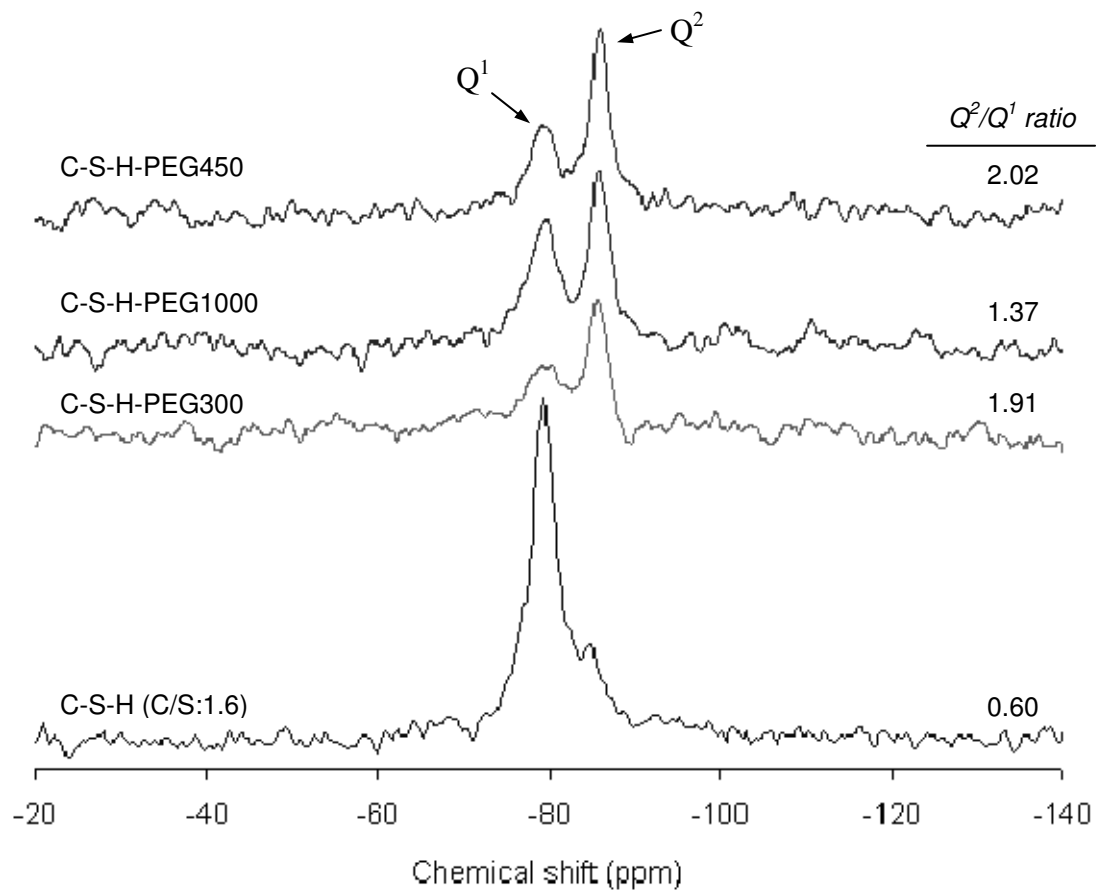


Figure 7

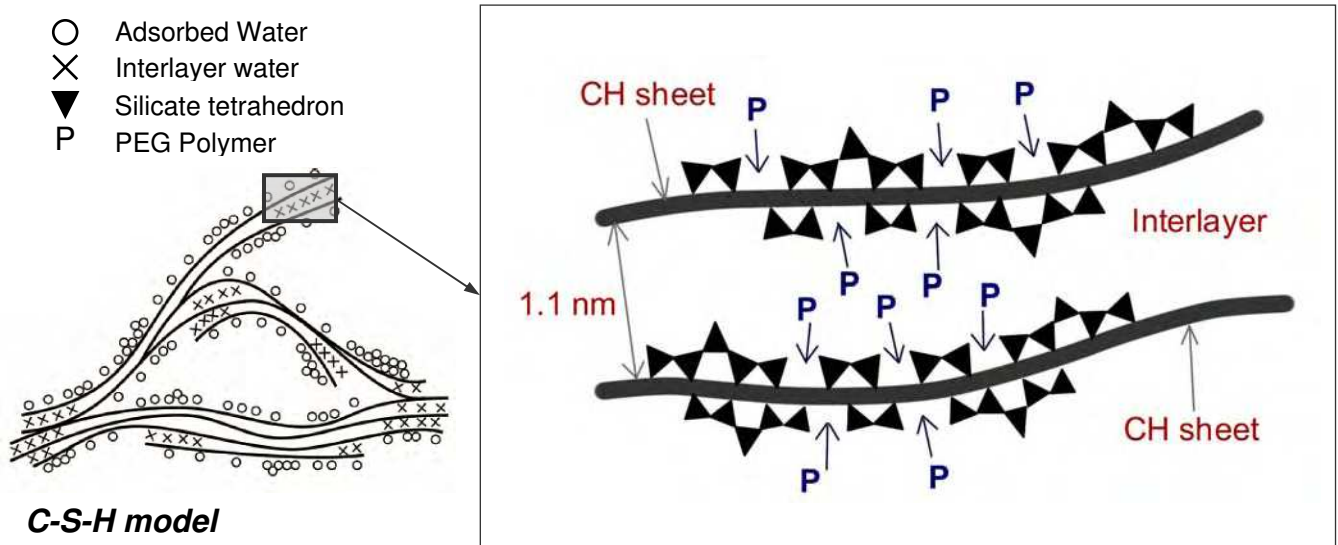


Figure 8

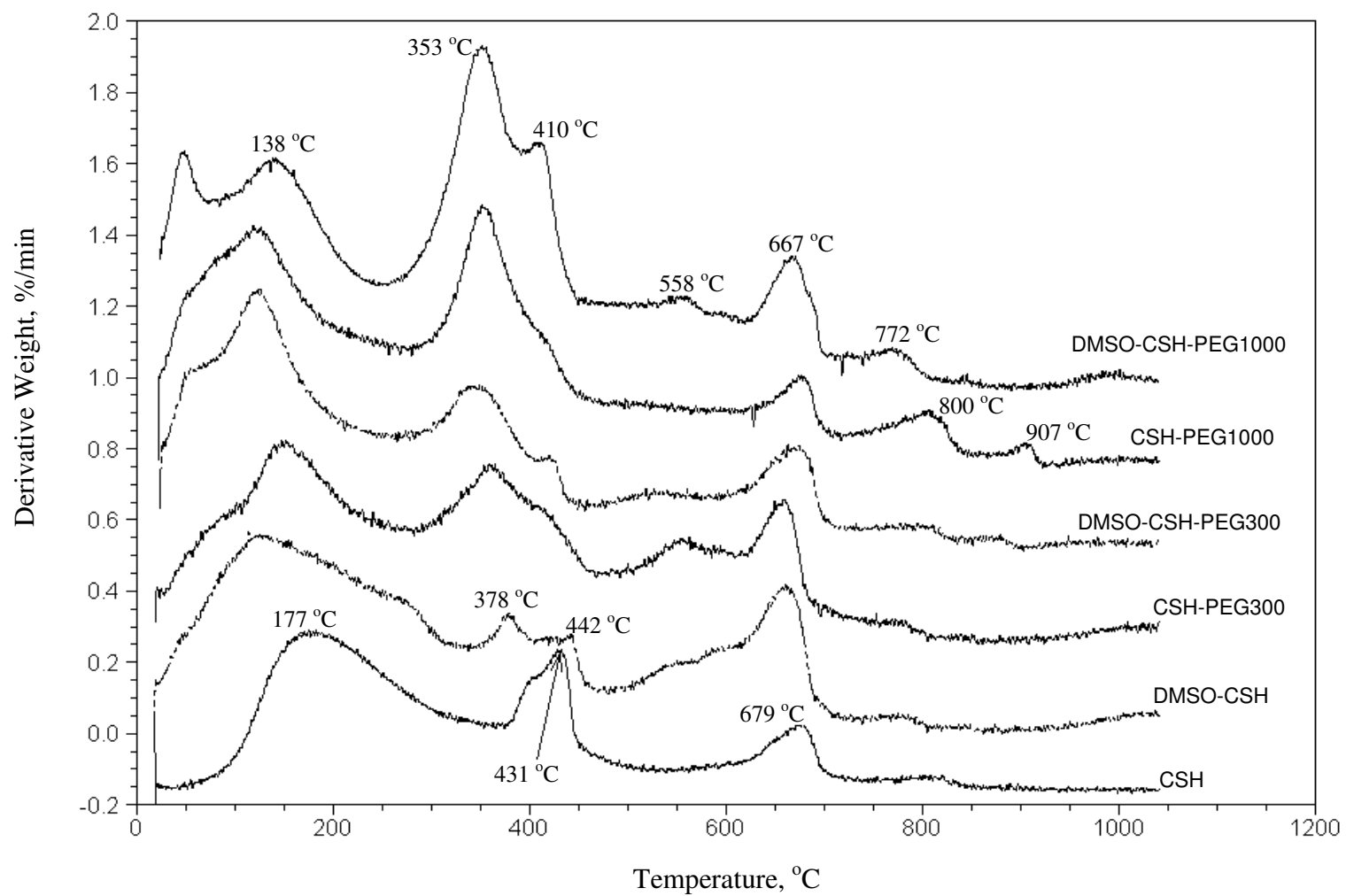


Figure 9